2012

Non-Intrusive Fault Detection in Reciprocating Compressors

Christopher James Schantz
cschantz@mit.edu

Steven Leeb

Non-Intrusive Fault Detection in Reciprocating Compressors

Christopher SCHANTZ[1]*, Steven LEEB[2]

[1,2]Massachusetts Institute of Technology, Research Laboratory for Electronics;
Laboratory for Electromagnetic and Electronic Systems, Cambridge, MA, USA
[1]cschantz@mit.edu, [2]sbleeb@mit.edu

*Corresponding Author

ABSTRACT

This research presents techniques developed for non-intrusive sensing and fault detection in reciprocating compressors driven by induction motors. These procedures are "non-intrusive" because they rely only on voltage and current signals measured on the compressor power cable. The electrical sensor based method allows for easy and non-intrusive determination of many fault sensitive signals that usually require complicated, expensive, and time consuming operations to measure. The electric signals are processed and used with the inverted dynamic motor model equations and motor parameters (which are also determined non-intrusively) to recover the instantaneous angular speed of the compressor shaft, as well as the torque of electromagnetic origin provided by the motor. These two intermediate signals and compressor parameters such as crank shaft inertia are then used to solve for the compressor load torque. This load torque signal has high fault diagnostic value because it is composed of pressure and friction torques, and these signals are close to mechanical phenomena of diagnostic interest in the compressor. All these signals are recovered at a fine resolution giving high level of detail on a sub-shaft revolution basis.

The use of the load torque signal in determining faults and additional diagnostic information is also given. A procedure for determining the cylinder suction and discharge pressure from the load torque signal and knowable cylinder parameters such as cylinder volume, crank arm length, and gas coefficients is discussed. The load torque signal is also useful directly: for the two piston machine used in the research, symmetry of the twice per rotation peak of the load torque is a valuable diagnostic measure. Reed valve leakage faults were investigated by drilling small holes of varying sizes in one cylinder's suction reed. The asymmetry in each cylinder's pressure torque peak increases with increasing leak size, providing both an indication and measure of leakage severity.

1. INTRODUCTION

Reciprocating compressors are widely used in industry. Healthy valves are vital for compressors to perform efficiently. Compressor valves are just one of many compressor components that, in general, are not easily accessible for inspection of their condition. This has led to a large body of research on indirect methods of sensing the health of compressors and their valves. Vibration based methods (McCarthy 1994) require the installation of vibration measurement devices in industrial or other non-ideal environments, as well as much skill in interpreting the resulting signals. We propose to use the electric signals measured on the power cable of the compressor's drive motor to determine mechanical faults for multi-cylinder compressors. The use of rugged and easy to install electric sensors that can be located away from the working environment of the compressor makes the method non-intrusive and reduces the cost of the fault detection method over common vibration-based methods. A basic description of the reciprocating compressor as it relates to the fault detection algorithm, followed by a short description of our experimental setup, rounds out this introductory section. The following three sections describe how the algorithm works and the steps required to convert the sampled electric signals into useful diagnostic information. Mathematical notation is kept to a minimum, see Schantz (2011) for in depth equations and a complete computer code implementation of the algorithm. The final sections of the paper describe the results of the fault detection algorithm when applied to a realistic refrigeration loop containing known valve faults. Estimates of cylinder suction and discharge pressures from this system are also presented and compared to known values.

1.1 Framework and Experimental Hardware

The reciprocating compressor is a time-variant nonlinear switched system with multiple inputs and outputs and many states. A schematic illustration of a reciprocating compressor is shown in Figure 1. An electric motor drives

the crank shaft of the reciprocating compressor, which causes motion of the pistons. The pistons act to compress gas by positive displacement, while the valves permit gas flow into and out of the cylinders so as to cause a pressure increase in the gas across the device. Our fault detection approach divides the compressor into three major subsystems important to its operation: the first subsystem is the induction motor, the second is the mechanical motion of the crankshaft and reciprocating pistons, while the third consists of the gas dynamics governed by the compressor's valves. Starting with the electric signals, the algorithm processes the signals through each domain using simplified models to create derivative signals of fault diagnostic value. The derivative signal outputs of each subsystem are then used as the input signals for the next subsystem, revealing more information at each stage. In addition, the intermediate signals often allow for verification of the simplifying assumptions of the models of the following stage, providing a valuable check on the accuracy of the results. For example, an indication of valve leakage by the algorithm would imply that the idealized healthy valve assumption of cylinder pressure estimator is invalid, preventing the user from being misled.

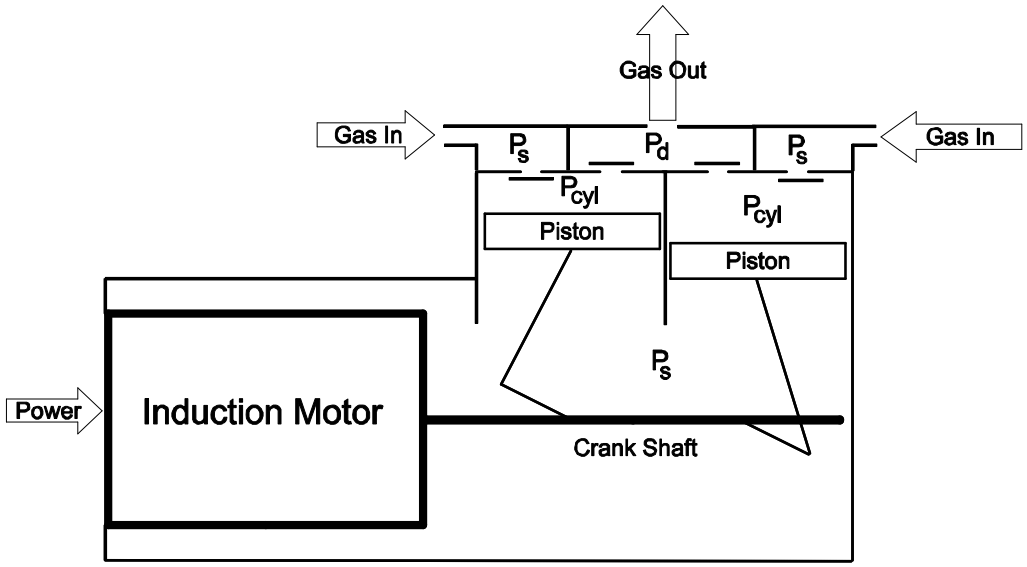

Figure 1: Functional components of a reciprocating compressor.

Two Copeland Corporation KAMA-007A-TAC-800 model compressors were used in this research. One compressor is installed in a research air conditioner, while the other compressor has been modified with an external shaft extension passing through the compressor case to allow installation of a 2500 count optical shaft encoder for precision speed measurement. Parameter fitting and fault detection experiments were conducted with the two compressors to develop and validate the fault detection algorithm. The compressor is a semi-hermetically sealed vertical cylinder design with two pistons linked 180 degrees apart on the crank shaft. The compressor is powered by a three-phase, four-pole induction motor directly connected to a 208 volt electric service. Complete electric measurements on the compressor require three voltage sensors and three current sensors. The sample rate must be fast compared to the shaft speed of the compressor in order to catch phenomena on time scales shorter that the shaft rotation. For the lab machine a sampling rate of 7 kHz was sufficient. A custom compressor head and valve plate described in Laughman (2008) allows direct sampling of cylinder pressure via two pressure sensors. Signals from these pressure sensors were used for algorithm validation and fitting of compressor model parameters.

2. ESTIMATING MOTOR IAS AND TORQUE FORM ELECTRICAL SIGNALS

Our algorithm is able to recover compressor shaft speed information without requiring difficult installation of shaft encoders as in the fault detection method of Al-Qattan *et al.* (2009) and Elhaj *et al.* (2010). The calculation of the instantaneous angular speed (IAS) $\dot{\theta}$ and torque $\tau_m$of the induction motor from the sampled electric signals v_s and i_s represents an inversion problem and is presented in equations (1-4). The remaining symbols of (1-4) are derived signals or motor parameters. There are two challenges in doing this. Obtaining accurate motor parameters is important, but the primary challenge is the fact that inverse problems in general are very sensitive to noise present in all sampled signals. . The algorithm to solve this problem is described below and in Schantz (2010) and covered in depth in Schantz (2011).

The algorithm removes the majority of the noise in the electrical signals by sampling for a duration of 150-300 shaft rotations, converting the signals to a rotating reference frame synchronous with the electric supply frequency, and then performing a synchronous averaging keyed to the shaft rotation. This averaging requires knowledge of the mean shaft speed, which is easily obtainable from the sampled signals (Schantz 2011). The synchronous averaging step acts like a comb filter (Braun 2011) and removes frequency components that are not harmonics of the fundamental shaft rotation frequency. This removes enough noise from the signals to allow numerical solutions to the induction motor inverse problem. Synchronous averaging to remove noise is justified because the induction motor subsystem, in contrast to the large compressor, is a time-invariant contracting system for the sampling durations involved (Schantz 2011). As proven by Lohmiller and Slotine (1998), the output of any time-invariant contracting system driven by a periodic input tends exponentially to a periodic signal with the same period. In the supply synchronous reference frame, the periodic load torque represents the only non-constant input to the induction motor, hence stator current signals ideally consist of content at the shaft rotation fundamental and its harmonics, while the supply voltage signals are ideally constant. Content not at these harmonics is considered noise. High frequency content above the 15th harmonic is also more likely to be noisy, and is removed with a low pass filter.

$$\lambda_{sk} = \frac{\boldsymbol{\mathcal{F}}(v_s - R_s i_s)}{j(k\omega_o + \omega_e)} \tag{1}$$

$$\lambda_{rk} = \frac{L_{ar}\lambda_{sk} - D\,\boldsymbol{\mathcal{F}}(i_s)}{L_m} \tag{2}$$

$$\dot{\theta} = \frac{2}{P}\left(\frac{\dot{\lambda}_r + R_r\boldsymbol{\mathcal{F}}^{-1}\left(\frac{L_m\lambda_{sk} - L_{as}\lambda_{rk}}{D}\right)}{j\lambda_r} + \omega_e\right) \tag{3}$$

$$\tau_m = \frac{L_m P}{2D}\mathbf{Im}\left(\bar{\lambda}_s\lambda_r\right) \tag{4}$$

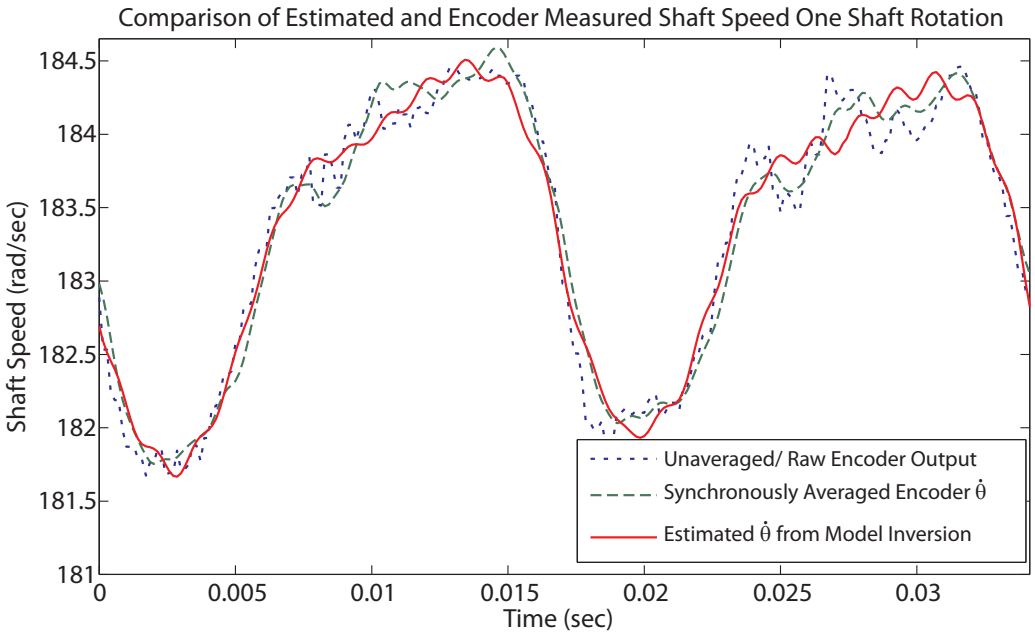

Figure 2: Comparison of estimated shaft speed with measured shaft speed for one typical cycle. Also included is the measured shaft speed averaged over the same duration as the electrical inputs used to estimate the shaft speed.

The problem of acquiring accurate motor model parameters is solved via a nonlinear minimization technique available in commercial computation packages. The particular optimizer employed for nonlinear minimization is described by Coleman and Li (1994) and (1996). The parameter fitting method is based on two key observations. The first is that the result of the inversion calculations using the correct parameters will produce a physically

meaningful (i.e. real) IAS signal, while parameter error will result in a significant imaginary part to the calculated IAS. The second observation is that the mean of the IAS signal be equal to the known mean shaft speed determined earlier for synchronous averaging. Minimization of an error function based on these ideas results in accurate parameter estimates and accurate IAS estimates. An example of typical good agreement between IAS estimates generated by our algorithm and directly measured IAS of a reciprocating compressor via shaft encoder is given in Figure 2.

3. CALCULATION OF LOAD TORQUE AND CYLINDER PRESSURE MODELING.

This section describes how the algorithm treats the two remaining subsystems of the compressor; the dynamics of the reciprocating mechanism and refrigerant compression. The major idea is to use the equation of motion of the mechanism shown in (5) along with estimated IAS ($\dot{\theta}$) and motor torque τ_l to solve for the load torque τ_l, which consists of gas compression pressure torque and frictional losses. Here we take a simplified approach to the equation of motion. Centripetal forces are insignificant for the shaft speeds involved, and the angular dependence of the generalized inertia parameter is also ignored, as the forces involved are small in comparison to the pressure loads on the pistons. This is also true of gravity effects. The generalized inertia is a function of crank shaft rotational inertia, crank arm and con rod length, and piston mass, all values easily known by manufacturers. For our experiments a combination of name plate data, disassembled component measurement, and least squares fitting from experimental data was used to set the generalized inertia parameter. It should be noted that knowledge of the generalized inertia is optional for the purposes of valve fault detection.

$$\tau_l = \tau_m - \mathcal{J}\ddot{\theta} \tag{5}$$

The quantities τ_m and $\dot{\theta}$ are known from the induction motor inversion procedure described earlier. Calculation of τ_l requires the differentiation of $\dot{\theta}$ to obtain $\ddot{\theta}$, and this has presented no problem if the low pass filter was used to remove high frequency noise in the electric signals as suggested in the previous section. The load torque is directly useful for fault detection and diagnosis as shown in section 5, or it may be used to determine the cylinder suction and discharge pressures. To obtain this information, the load torque must be processed through a model of friction and cylinder pressure torques, which are described next.

3.1 Simplified Cylinder Pressure Model

The simplified cylinder pressure model assumes that the valves are mass-less: they open or close instantly when the pressure difference across them changes sign, and the valve flow areas offer no resistance to flow. Compression is governed by the polytropic compression model. For a piston cycle beginning after the discharge valve has closed at top dead center the refrigerant gas remaining in the cylinder clearance volume expands as the piston drops. When the cylinder pressure drops below the suction plenum pressure, the suction valve opens equalizing pressures and remains open until the piston starts to rise again. Then compression occurs until the cylinder pressure becomes greater than the discharge pressure, once again opening a valve and causing pressure equalization with the discharge plenum. The discharge valve closes when the piston reaches top dead center and the cycle repeats.

The simplified cylinder pressure model is required because a more complicated model containing valve dynamics such as flutter and impact would have a large number of parameters which would decrease the stability of any algorithm that calculates cylinder pressure from the load torque signal. In addition, compressor manufactures strive to create valves that behave in exactly the idealized matter assumed by the simplified model. For comparison a plot of cylinder pressures expressed by the simplified model are overlaid on measured cylinder pressures in Figure 3. The plot was generated by finding the best fit p_s, p_d, clearance volume V_{clear}, and polytropic exponent k to match measured cylinder pressure. Note that the plot is not an output of the fault detection algorithm. Generation of these best fit suction and discharge pressures is needed to evaluate the accuracy of the cylinder pressure estimator due to the complicated nature of the true cylinder pressures while gas is flowing through the valves.

Since V_{clear} does not vary with operating condition and k only varies weakly, the values of these parameters are assumed to be a priori information available for the fault detection algorithm. For the purpose of finding other compressor parameters, the cylinder pressure model just described can be used to calculate the force on the pistons and the torque on the crank shaft due to cylinder pressure. Knowing this pressure torque, the time derivative of the IAS, and the torque developed by the induction motor allows a least squares estimation of the friction coefficients

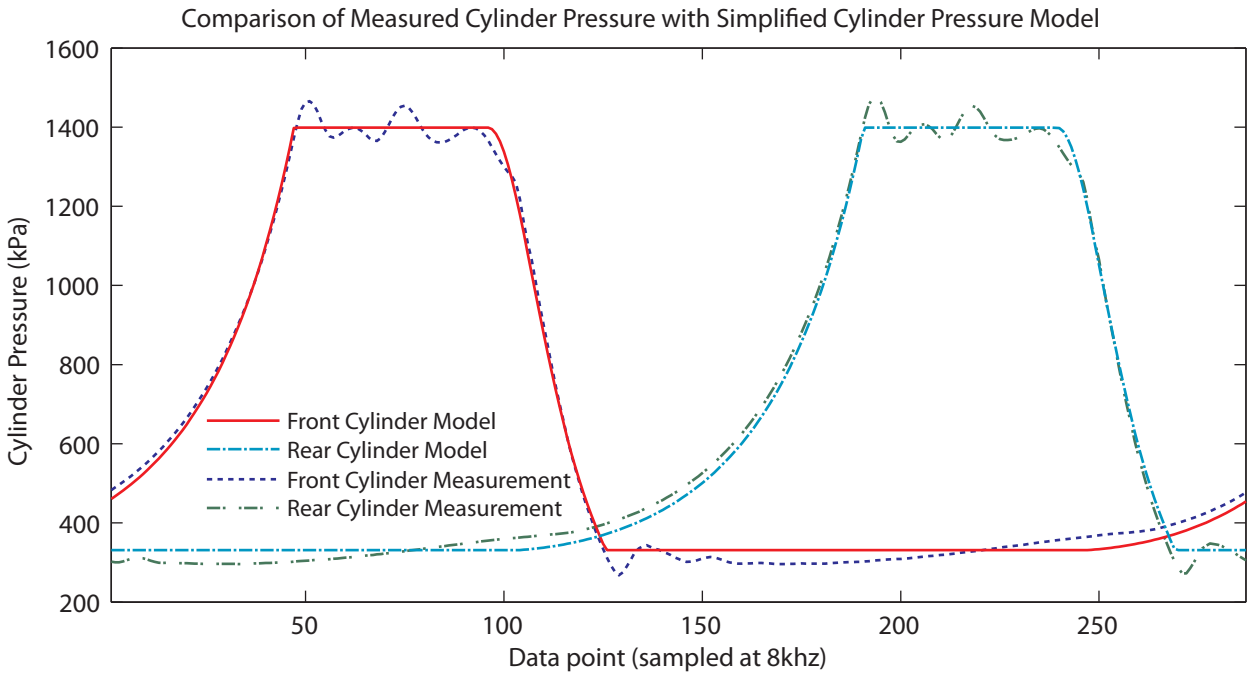

Figure 3: A comparison of the simplified cylinder pressure model with measured cylinder pressures.

that govern the friction losses. Only the crank shaft bearing friction and the piston sliding friction were considered important. However, the pressure and friction forces on the piston act on the crank shaft through the same lever arm and cannot be distinguished in a crankshaft torque balance. This causes the least squares estimate of the piston friction coefficient to be sensitive to any approximation error inherent in the simplified cylinder pressure model. The result is that the estimated piston sliding friction coefficient may be negative. This poses no problem and incorporating this negative value increases the accuracy of the cylinder operating pressure estimator.

4. ALGORITHM FOR SUCTION AND DISCHARGE PRESSURE ESTIMATION

The recovered load torque signal τ_l, along with known cylinder pressure and friction model parameters, contains enough information to produce an estimate of the compressor operating pressures. Unlike a compressor energy balance that is able to provide a rough estimate of the pressure difference across the compressor, the pressure determination procedure here results in an estimate for the suction and discharge pressures in the cylinder. This information makes the load torque signal useful for fault detection of the larger system in which the compressor is located. The main difficulty is that the estimated load torque signal is not referenced to a known crank angle, while the contribution to load torque by the cylinder pressure and friction forces depend strongly on crank angle.

The algorithm calculates load torque curves $\hat{\tau}_l$ as a function of candidate $\hat{P}_s$ and $\hat{P}_d$ values and minimizes the error (or difference) between $\hat{\tau}_l$ and τ_l, in a numerical minimization procedure. In order to meaningfully compare $\hat{\tau}_l$ and τ_l, the torques must be expressed relative to a common crank angle. The crank angle of $\hat{\tau}_l$ is known from the cylinder pressure and friction models from which it was generated, but the crank angle of τ_l is unknown. Periodic cross correlation provides the solution. The time shift resulting in maximum correlation between $\hat{\tau}_l$ and τ_l is assumed to bring both signals to a common crank angle. It is important to ensure that there is one clear point of maximum correlation between $\hat{\tau}_l$ and τ_l otherwise the cross correlate and shift operation can destabilize the minimization procedure. The assumption of healthy cylinders means that the load torque signals are periodic with each cylinder's contribution matching any other cylinder's contribution, causing many points of strong correlation between $\hat{\tau}_l$ and τ_l, one for each cylinder. However, any differences between each cylinder's contributions to τ_l are assumed to be caused primarily by noise. Stability can be improved by folding and averaging each cylinder's load torque contribution into a single characteristic load torque curve. This allows the minimization to iterate stably until termination resulting in estimates of the cylinder operating pressures. A block diagram of the algorithm is given in

Figure 4 below. Extensive derivations of the models and algorithms involved, along with example code for the numerical procedures are given in Schantz (2011).

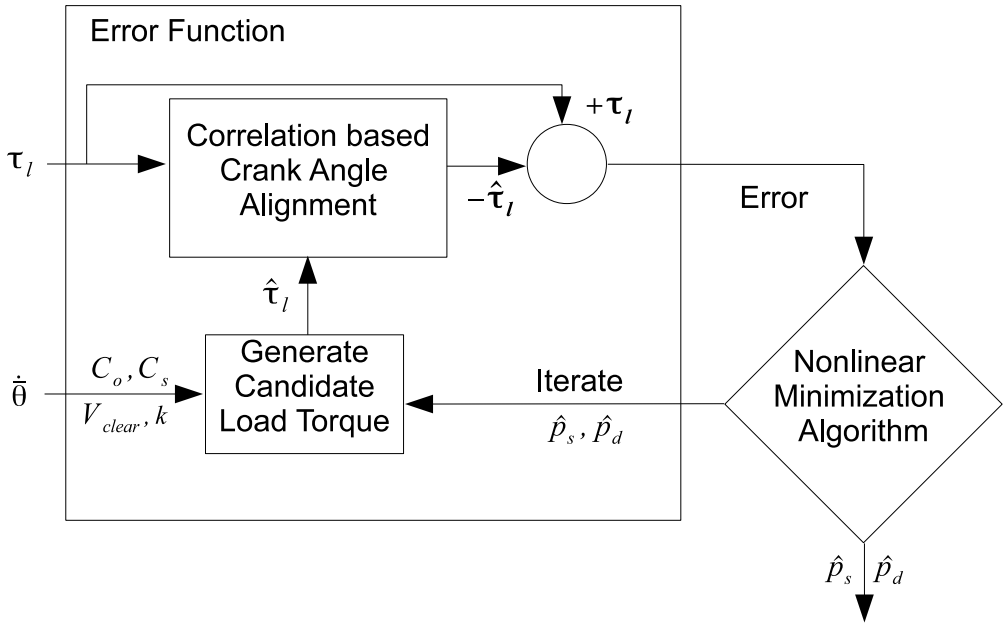

Figure 4: Flow chart of the algorithm to estimate cylinder pressures from the load torque signal.

5. VALVE FAULT EXPERIMENT AND RESULTS

Correct operation of a compressor's valves is important for efficient functioning of the compressor. The spectrum of valve damage severity is large and, in some cases, can be extremely hard to notice. Common reasons for valve damage include attempted compression of an incompressible liquid such as condensed refrigerant or oil or interaction with solid debris. Solid debris in the refrigeration loop (that has been cited as the cause of valve damage) is usually composed of slivers of metal left over from manufacture or installation of the system (Glaeser 1999). Damaged valves do not effectively seal the cylinder from the suction or discharge manifolds. The undesired flow of refrigerant through these leaks represents a loss of volumetric efficiency for the compressor (Breuker and Braun 1998). As a fault resulting in degraded compressor efficiency, minor leaks caused by valve faults are an important target for detection in any fault detection method.

Previous compressor fault detection studies have simulated valve faults by installation of a refrigerant bypass path between the suction and discharge sides of the compressor. A valve is installed on this line and the flow area is varied to simulate various valve faults (Armstrong 2004), (Armstrong *et al.* 2004). The compressors used in the present research have reed-type suction and discharge valves. Glaeser (1999) studied the failure mechanisms of reed valves in refrigeration compressors and gave photographs of failed reed valves. These photographs were used as a guide to intentionally damage suction reeds in a functionally similar manner. In this research, valve faults were simulated directly by drilling holes in suction reeds and installing the reeds in the compressor. The compressor was part of a laboratory air conditioner system. After each valve installation, the system was re-charged with refrigerant and allowed to run for approximately 5-10 minutes before a one minute period of voltage and current data was recorded for processing by the fault detection method. Cylinder pressure measurements were also collected with high dynamic range pressure sensors installed in the compressor head plate to assess the severity of the leak on the cylinder pressure, and validate the physical mechanism behind the fault detection method.

The four tested conditions corresponded to a fault-free baseline and three faulty suction reeds of increasing leak size. These holes were drilled in the region of the reed that seals the cylinder from the suction manifold of the compressor. Photographs of the "damaged" suction reeds are shown in Figure 5. The reeds were installed in the compressor valve assembly shown in Figure 6a and Figure 6b.

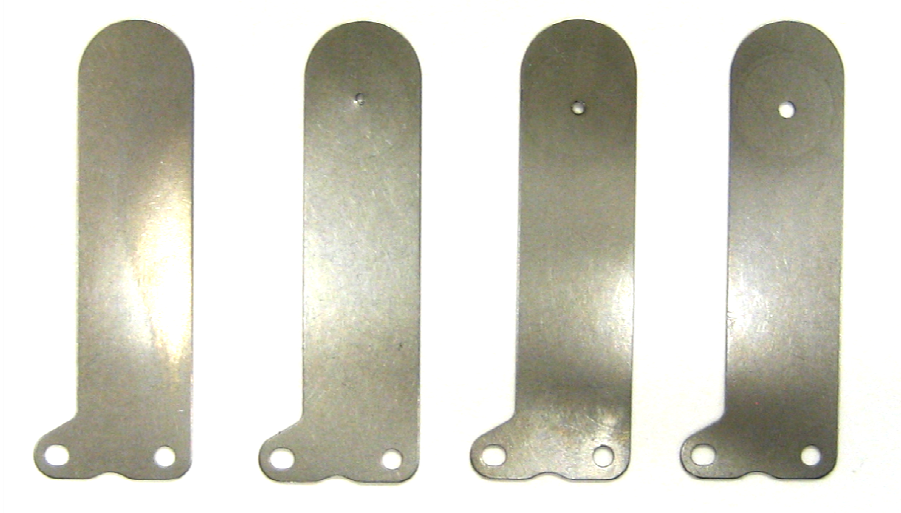

Figure 5: Suction reeds. Leakage size from right to left: 0mm^2 baseline, 0.8mm^2, 1.5mm^2, and 3.1mm^2.

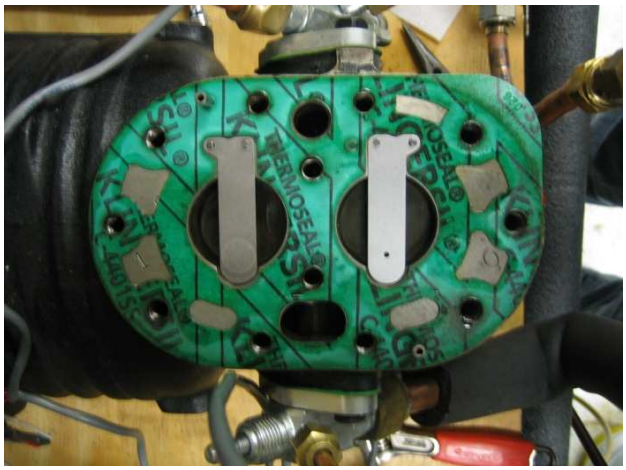

Figure 6a: Suction reeds installed in compressor without valve plate.

Figure 6b: Suction reeds installed in compressor with valve plate.

The output of the fault detection method most sensitive to valve faults and other mechanical faults within the compressor is the load torque curve. The normalized load torque curves for the four valve fault conditions are shown in Figure 7 with the convention that positive load torque accelerates the crankshaft. Each region of the load torque curve can be associated to a particular piston due to the dominant contribution of that piston's pressure torque during the compression and discharge phase of its cycle. In Figure 7 each piston's load torque region is superimposed. Below each load torque subplot is the measured cylinder pressure from each test confirming the presence of the leak.

Referencing Figure 7, the two regions of the load torque curve are expected to appear similar to each other if the valves and other components of each cylinder are operating in identical (healthy) condition. This is true for the top left plot of Figure 7 which represents the baseline case. For the fault cases this is not true, and the degree of dissimilarity increases with the severity of the fault. It is clear that valve leaks reduce the pressure in the affected cylinder, which is reflected in the reduced load torque on the crank shaft when the affected cylinder undergoes compression. An example metric that easily captures the dissimilarity between load torque regions associated with each piston is the difference in area enclosed by each curve. Table 1 contains this metric for each case. Only suction valve faults were tested due to the ease of replacement of the suction reeds. The fault detection method should be sensitive to discharge valve faults and other leaks, such as gasket or seal leaks, using an identical procedure. A necessary assumption for this procedure is that the fault affects one cylinder to a greater degree than the other

cylinder, or pre recorded baselines at known operating conditions can be compared against to detect faults that affect each cylinder equally.

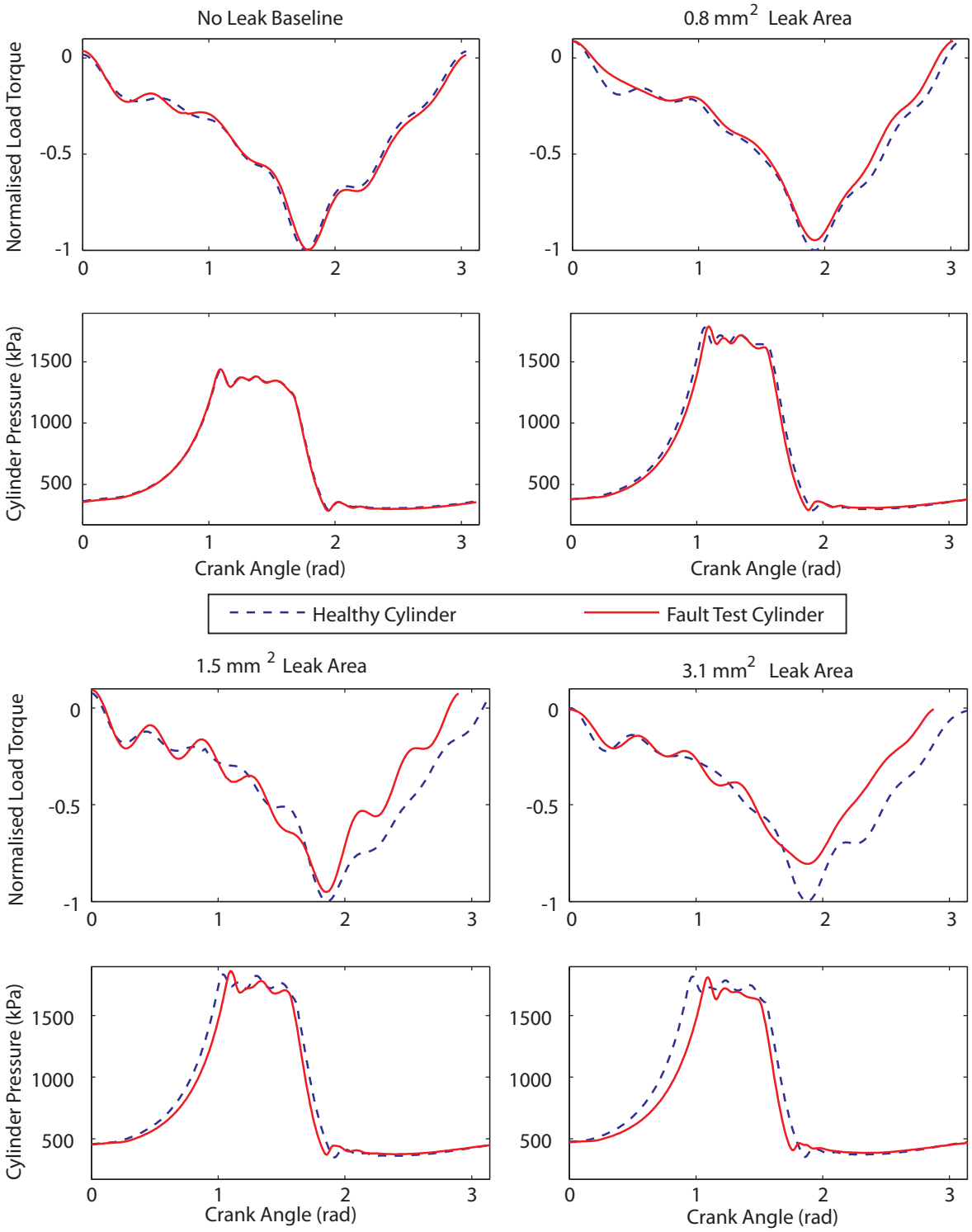

Figure 7: Comparison of normalized load torque signals and cylinder pressure measurements for each test (top and bottom plot of each pair respectively). The solid line represents the cylinder with the valve leakage fault. The dashed line is data from the healthy cylinder.

Table 1: Presentation of the simple fault detection metric for valve leakage faults. Severity of the fault is ratio of suction reed leakage area to total suction port area of 60 mm^2.

Suction Reed Leak Area	Fault Severity	Fault Detection Metric
Baseline (no hole)	0	0.74
0.811 mm^2	0.014	5.46
1.533 mm^2	0.025	8.66
3.093 mm^2	0.052	11.92

6. CYLINDER PRESSURE DETERMINATION RESULTS

The load torque signal is sensitive to the loads on the crankshaft of the compressor, such as the torque going into compression of the refrigerant. It is possible to estimate the cylinder suction and discharge pressures from the load torque curve. An assumption required by the estimation algorithm is that the compressor cylinders are fault free. This requirement can be verified via the simple test on the load torque curve described in the previous section. The algorithm to generate cylinder pressure estimates was discussed in detail in Section 4.

A range of suction and discharge pressure conditions were generated in the instrumented air conditioner for testing of the pressure estimation algorithm. The various suction and discharge pressure conditions were created by immersing the temperature sensing bulb of the unit's thermal expansion valve (TXV) in a temperature controlled recirculating water bath. The temperature of the bath was varied in 3°C steps from 5°C to 23°C. At each temperature level the unit was operated for approximately 30 minutes to come to steady-state and allow the bath temperature to stabilize. Then a 30 second duration set of electrical measurements was recorded, along with pressure measurements for validation. The electrical measurements were processed by the fault detection algorithm to generate the load torque signal. The load torque signal was then input to the pressure estimation algorithm of Section 4 to generate estimates of the cylinder suction and discharge pressures. The results are presented in Table 2. The table also compares these estimates with some of the cylinder suction and discharge pressure definitions as discussed in Section 3.1. The comparative best fit pressure values were generated from the validating cylinder pressure measurements. The error between suction and discharge pressure estimates and the best fit (measured) suction and discharge pressures is less that 3% in for the tested conditions.

Table 2: Results of the cylinder pressure estimation algorithm compared with best fit pressures of the simplified cylinder pressure model and the measured cylinder pressure range.

Bulb Temp	Estimated Cylinder Pressures (kPa)		"Best Fit" Cylinder Pressures (kPa)		Measured Suction Pressure Range (kPa)		Measured Discharge Pressure Range (kPa)	
	Suction	Discharge	Suction	Discharge	Minimum	Maximum	Minimum	Maximum
5°C	258	1333	256	1370	208	286	1319	1457
8°C	285	1356	283	1389	229	292	1342	1470
11°C	306	1409	305	1395	249	337	1353	1473
14°C	325	1424	331	1399	270	363	1363	1469
17°C	343	1408	347	1406	286	383	1367	1477
20°C	356	1404	363	1409	299	396	1361	1480
23°C	372	1408	373	1413	305	407	1359	1490

7. CONCLUSION

Fault detection in reciprocating compressors using electrical measurements is experimentally demonstrated to be sensitive to leaking reed valves. The load torque signal of the crankshaft is calculated and asymmetry between the contributions of nominally identical cylinders serves as the fault indicator. Independently, a procedure is given to estimate cylinder suction and discharge pressures from the load torque signal to expand the prognostic capability of the non-intrusive method beyond the compressor itself. The mathematical foundations of the algorithm give promise for its use in a wide range of induction motor driven systems with a sufficiently periodic load torque, including most types of positive displacement compressors.

NOMENCLATURE

C_o	crank shaft friction coefficient	R_r, R_s	Resistance (rotor, stator)
C_s	piston friction coefficient	τ_l	load torque
D	$= L_m^2 - L_{ar}L_{as}$	τ_m	motor torque
i_s	stator current	θ	shaft angle
j	$j^2 = -1$	ω_e	electric supply frequency
$\mathcal{J}$	generalized inertia	ω_o	sampling frequency w.r.t. shaft rotation
k	Fourier transform frequency vector		Operators
L_{ar}	total rotor inductance	$\boldsymbol{\mathcal{F}}(\cdot)$	Fourier transform
L_{as}	total stator inductance	$\boldsymbol{\mathcal{F}^{-1}}(\cdot)$	inverse Fourier transform
L_m	motor magnetizing inductance	$\mathbf{Im}(\cdot)$	imaginary part
P	motor pole count	$\overline{(\cdot)}, \overline{(\cdot)_{\boldsymbol{k}}}$	mean, or complex conjugate
P_{cyl}, P_s, P_d	Pressure (cylinder, suction, discharge)	$\dot{(\cdot)}, \ddot{(\cdot)}$	single, double time derivative

REFERENCES

Al-Qattan, M., Al-Juwayhel, F., Ball, A., Elhaj, M., Gu, F., 2009, Instantaneous angular speed and power for the diagnosis of single-stage double-acting reciprocating compressor, *Proceedings of the Institute of Mechanical Engineers Part J Journal of Engineering Tribology*, vol. 223, no. 1, pp. 95–114.

Armstrong, P., 2004, *Model identification with application to building control and fault detection*, Ph.D. dissertation, Massachusetts Institute of Technology, Cambridge MA, 142 pages. http://dspace.mit.edu/handle/1721.1/28805

Armstrong, P., Laughman, C., Leeb, S., Norford, L., 2004, Fault detection based on motor start transients and shaft harmonics measured at the rtu electrical service, *International Refrigeration and Air Conditioning Conference at Purdue*, Purdue University, no. R137, pp. 1–10.

Braun, S., 2011, The synchronous (time domain) average revisited, *Mechanical Systems and Signal Processing*, vol. 25, pp. 1087–1102.

Breuker, M., Braun, J., 1998, Common faults and their impacts for rooftop air conditioners, *International Journal of HVAC+R Research*, vol. 4, no. 3, pp. 303–318.

Coleman, T., Li, Y., 1994, On the convergence of reflective newton methods for large-scale nonlinear minimization subject to bounds. *Mathematical Programming*, vol. 67, no. 2, pp. 189–224.

Coleman, T., Li, Y., 1996, An interior, trust region approach for nonlinear minimization subject to bounds, *SIAM Journal on Optimization*, vol. 6, pp. 418–445.

Elhaj, M., Almrabet, M., Rgeai, M., Ehtiwesh, I., 2010, A combined practical approach to condition monitoring of reciprocating compressors using IAS and dynamic pressure. *World Academy of Science Engineering and Technology*, vol. 63, pp. 186–192.

Glaeser, W., 1999, Failure mechanisms of reed valves in refrigeration compressors, *Wear*, vol. 2, pp. 918–924.

McCarthy, D., 1994, *Vibration-based diagnostics of reciprocating machinery*, Ph.D. dissertation, Massachusetts Institute of Technology, Cambridge MA, 181 pages.

Laughman, C., 2008, *Fault detection methods for vapor compression air conditioners using electrical measurements*, Ph.D. dissertation, Massachusetts Institute of Technology, Cambridge MA, 424 pages. http://dspace.mit.edu/handle/1721.1/45938

Lohmiller, W., Slotine, J., 1998, On contraction analysis for nonlinear systems, *Automatica*, vol. 34, no. 6, pp. 683–696.

Schantz, C., Remscrim, Z., Leeb, S., 2010, Electrical determination of reciprocating compressor instantaneous angular speed, *International Refrigeration and Air Conditioning Conference at Purdue*, Purdue University, no. R2474, pp. 1–7.

Schantz, C. 2011, *Non-intrusive Fault Detection in Reciprocating Compressors*, Master's thesis, Massachusetts Institute of Technology, Cambridge MA, 166 pages. http://dspace.mit.edu/handle/1721.1/67800

ACKNOWLEDGEMENTS

The authors would like to thank many people whose ideas, advice, and assistance have played a vital role in the completion of this research, specifically Zack Remscrim, Warit Wichakool, Jim Paris, Uzoma Orji, Jarred Schantz, Christopher Laughman, and Peter Armstrong. We also recognize the generous funding and support, vital for the conduct of this research, from The Grainger foundation, ONR's ESRDC Program, and NEMOmetrics.